Catalysis Letters
https://doi.org/10.1007/s10562-022-03980-x

Effect of Surface Hydroxyl Content of Support on the Activity of Cu/ZSM-5 Catalyst for Low-Temperature Hydrogenation of Dimethyl Oxalate to Ethylene Glycol

Hongfei Yun[1] · Yu Zhao[1,2] · Xian Kan[1] · Guixian Li[1,2]

Received: 10 February 2022 / Accepted: 9 March 2022
© The Author(s), under exclusive licence to Springer Science+Business Media, LLC, part of Springer Nature 2022

Abstract
Cu/SiO_2 catalyst prepared by the ammonia-evaporation (AE) method is the potential preferred catalyst for hydrogenation of dimethyl oxalate (DMO) to ethylene glycol (EG). Although significant advancements have been obtained in the confirmation and influence factors of active species in the hydrogenation process, the relationship between the catalytic activity and the sensitive factors in the preparation or pretreatment process of the catalyst is still uncertain. In this paper, Cu/ZSM-5 catalysts for DMO hydrogenation to EG were prepared by the AE method using ZSM-5 molecular sieve with high silicon-alumina ratio (1500) as a support. The ZSM-5 support was pretreated by drying at 393 K for different hours and it was found that the surface hydroxyl group of the support had significant influence on the structure and catalytic hydrogenation performance of the prepared Cu/ZSM-5 catalyst. The distribution of surface hydroxyl groups could be significantly changed by pre-drying the carrier, which further resulted in the change of the copper dispersion and surface properties of subsequent copper-supported catalysts. With the decrease of hydroxyl content on the surface of the ZSM-5 support, the prepared reduced Cu/ZSM-5 catalyst possessed smaller Cu^0 particles size, higher copper dispersion, higher surface area of Cu^0 and Cu^+ species, but weakened surface acidity of the catalyst, which resulted in the great improvement of the catalytic activity. The DMO conversion and EG selectivity could reach 100% and 93% even under the low reaction temperature at 448 K over the Cu/ZSM-5-24 catalyst (based on the ZSM-5 support pretreated by drying for 24 h). In addition, the catalytic activity did not show obvious change after 300 h of reaction, probably due to the low temperature reaction and suitable surface properties of the catalyst.

✉ Yu Zhao
yzhao@lut.edu.cn

✉ Guixian Li
lgxwyf@163.com

[1] Present Address: School of Petrochemical Engineering, Lanzhou University of Technology, Lanzhou 730050, Gansu, China

[2] Key Laboratory of Low Carbon Energy and Chemical Engineering in Gansu Province, Lanzhou University of Technology, Lanzhou 730050, Gansu, China

Published online: 24 March 2022

Graphical Abstract

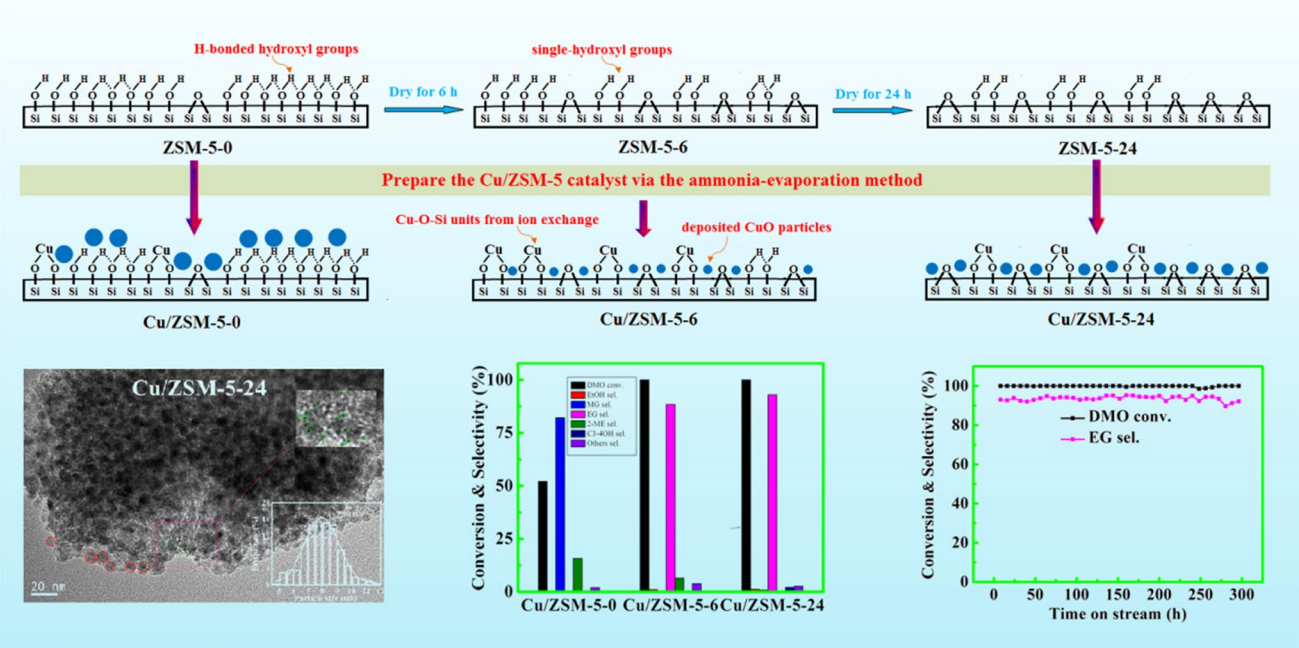

Keywords Surface hydroxyl group · Cu/ZSM-5 catalyst · Dimethyl oxalate · Hydrogenation · Ethylene glycol

1 Introduction

Ethylene glycol (EG) is an important chemical product and widely used to produce polyester fiber, antifreeze, etc. [1]. At present, ethylene oxidation is a universal industrial approach to produce EG. However, the indirect synthesis of EG from coal is considered to be the most valuable C_1-chemistry process both in the economic and environmental persistent development compared to the process of petroleum-derived EG [2]. The coal to EG process consists of two steps [1, 3]: firstly, gasification of coal to syngas and catalytic coupling of CO with nitrite esters to DMO, which has been industrialized [4]; then, the hydrogenation of oxalates to EG, which is suffered from the toxic copper-chromium catalyst.

Teunissen et al. [5] have investigated the Ru-based homogeneous catalysts in the hydrogenation of DMO and EG yield of 95% was obtained under the conditions of 7 MPa and 373 K. Considering the problems of equipment corrosion and product separation in homogeneous hydrogenation, an efficient production of EG from the heterogeneous hydrogenation technology of DMO was developed. Copper-chromium catalysts have been the preferred industrial catalysts for the coal-to-EG process because they possess relatively high catalytic activity and long lifespan. Nonetheless, the chromium oxide is toxic, which restricts its wide applications. Therefore, the chromium-free Cu-based catalysts have been extensively studied. Different carriers [6–12] have been chosen to prepare copper-based catalysts for hydrogenation of DMO. However, the acid or base sites of the supports will lead to produce more by-products that will decrease the selectivity of target product EG [9, 13]. Thus, copper-silicon catalyst was found to exhibit outstanding performance in the hydrogenation of DMO due to the weak acidic and basic properties of SiO_2 [6, 14, 15]. In addition, Xu et al. [16] reported that the Cu–O–SiO_x interface creates an exceptional effect to promote catalytic hydrogenation of esters by stabilizing the transition states of Cu–$H^{\delta-}$ and SiO–$H^{\delta+}$ species.

In the catalytic process of Cu based catalysts, it is generally accepted that the synergistic effect of Cu^0 and Cu^+ species is the key to catalyze the hydrogenation of DMO to EG, and the synergistic catalytic mechanism of Cu^0 and Cu^+ species in ester hydrogenation has been illustrated through experiments and theoretical calculations, that is, the Cu^0 species dissociatively adsorbs H_2, while the Cu^+ species promotes the active adsorption of methoxyl or acyl groups in ester molecules, and the dissociation adsorption of oxalate is the rate-controlling step of the reaction [17]. Therefore, the content of Cu^+ in the catalyst is the most direct factor affecting the hydrogenation of DMO [18]. Generally, methods such as preparation of copper

phyllosilicate [1, 14], utilization of oxygen vacancies of the carrier [19, 20], or addition of promoter [21–23] are used to increase the content of Cu^+ in the catalyst.

Ammonia evaporation (AE) method is widely used to prepare Cu/SiO_2 catalysts, during which a very important ion-exchange reaction occurs [24]. Ding et al. [25] found that more stable and higher activity Cu^+ species was obtained through the ion exchange of copper ammonia complex with surface hydroxyl groups of SiO_2 support. For Cu/SiO_2 catalyst, one of the current troublesome problems is that the catalyst activity will change greatly under the influence of some unknown factors and the catalytic activity is extremely sensitive to the preparation process, storage environment and storage time of the catalyst. In this paper, Cu/ZSM-5 catalyst was prepared through the AE method using ZSM-5 zeolite with high silica-alumina ratio as support. Choosing the ZSM-5 zeolite as the probe support was based on the consideration that its strong acidic sites from the bridge hydroxyl group (Al–OH–Si) can be turned into the medium strong and weak acidic sites with the elimination of aluminum hydroxyl groups during the drying process, which is favorable to the study of the effect on the acid site of the catalyst. It was found that the change of hydroxyl group on the surface of the support has a significant influence on the catalytic performance of the prepared Cu/ZSM-5 catalyst, and what's more, the change of hydroxyl group on the surface of carrier can occur during the common drying operation, which is often completely ignored by the researchers. The conclusion in this paper will be of great significance to the technological progress in the field of Cu-based catalyst.

2 Experimental

2.1 Materials

HZSM-5 (Si/Al = 1500), Shandong Hefa Environmental Protection Technology Co., LTD. $Cu(NO_3)_2{\cdot}3H_2O$, A.R., Tianjin Damao Chemical Reagent Factory. Ammonia, A.R., 25–28 wt% NH_3, Yantai Shuangshuang Chemical Co., LTD. Methanol, A.R., Lean Long bohua (Tianjin) Pharmaceutical & Chemical Co., LTD. All the reagents and solvents are commercially available and without further purification prior to use.

2.2 Catalyst Preparations

ZSM-5 zeolite was dried at 393 K for 0, 6 and 24 h, respectively.

25%Cu/ZSM-5 were prepared by ammonia evaporation method. Specially, 15.22 g of Cu $(NO_3)_2{\cdot}3H_2O$ was dissolved in 300 ml of deionized water. 50 ml of 25% ammonia aqueous solution was added and stirred for 0.5 h. The initial pH of the suspension was 11–12. Then 12 g of ZSM-5 after drying was added to the copper-ammoniacal complex solution and ultrasonic dispersion for 1 h. After stirring for 4 h at room temperature, the suspension was heated to 363 K to evaporate ammonia in a water bath until the pH value of the suspension decreased to 6–7. The precipitate was washed with deionized water and dried at 393 K overnight. The catalyst precursors were calcined at 723 K for 4 h, and denoted as Cu/ZSM-5-N, where N represents the dry temperature of carrier.

2.3 Catalyst Characterization

The BET surface area, pore volume, and average pore diameter of the catalysts were determined by N_2 physical adsorption at liquid nitrogen temperature using a Quantachrome NOVA 2200E instrument. The sample was degassed at 523 K for 2 h in vacuum before analysis to remove the physically adsorbed components.

The actual copper content of the samples was determined by inductivity coupled plasma optical emission spectrometry (ICP-AES) on the Varian ICP-OES 720 unit.

FT-IR spectra of the catalyst samples were recorded on Nicolet Nexus 670 using the standard KBr disk method. The spectra region was recorded from 4000 to 400 cm^{-1} by averaging 32 scans with resolution ratio of 4 cm^{-1}.

The phase composition and particle size of the catalyst were determined using Cu-Kα radiation (λ = 1.5406 Å) on a Rigaku Ultimate IV XRD diffractometer. The tube voltage was 40 kV, and the current was 40 mA. The scanning speed was 4°/min from $2\theta = 10°$ to $2\theta = 90°$. The Scherrer equation was used to calculate the particle size of the copper species.

Transmission electron microscope (TEM) images were obtained by a Philips TECNAI G2 F20 system electron microscope.

The reduction behavior of solid catalysts was investigated by H_2-TPR method on AutoChem II 2920. The calcined samples were dried for 0.5 h in 393 K. Ar atmosphere and then cooled to room temperature. Then the samples were heated to 673 K in the flow of 10% H_2–Ar with a heating rate of 10 K/min. The amount of hydrogen consumption was determined by a thermal conductivity detector (TCD). The metallic Cu surface area was measured by N_2O titration [3].

The surface acidity of the catalysts was measured by the NH_3-TPD method. The samples was reduced for 2 h at 583 K in a H_2/Ar atmosphere (1/9, V/V, 50 ml/min) and then purged for 2 h with a high-purity He flow (50 ml/min) at 583 K. When the temperature cooled down 373 K, ammonia gas was introduced until saturation, and then the sample was sweeped with He flow (50 ml/min) for 90 min. Finally, the sample was heated from 323 to 973 K at a rate of 10 K/min, and the released NH_3 was monitored by mass spectrometer.

X-ray photoelectron spectra (XPS) and Auger electron spectroscopy (XAES) were carried out to analyze copper species on a PHI 1600 ESCAinstrument (PE Company) equipped with an Al Kα X-ray source (hν = 1486.6 eV). Before testing, the samples was reduced in a flow of H_2 at 573 K for 4 h and then cooled to room temperature. The binding energy or kinetic energy of Auger electron was corrected with C 1 s peak of 284.6 eV as reference.

2.4 Catalytic Performance Tests

The catalytic performance was tested in a miniature fixed-bed reactor. The steps are as follows: The Cu/ZSM-5-N catalyst was packed into a stainless steel reactor (inner diameter = 8 mm). Firstly pre-reduced in a stream of pure hydrogen at 573 K under atmospheric pressure for 4 h with a flow rate of 50 ml/min, and then the catalyst bed was cooled to the 448 K. After that, adjust the system pressure to 2 MPa, then the 10% dimethyl oxalate methanol solution was injected into the reactor by high pressure pump continuously with a H_2/DMO molar ratio of 120. The weight liquid hourly space velocity of DMO ($WLHSV_{DMO}$) was varied from 0.10 to 1.10 h^{-1}. The liquid products were cooled, collected and analyzed by a gas chromatography equipped with a flame-ionization detector and 30 m HP-INNOWAX chromatographic column, in which 2-propanol was employed as the internal standard. The main products of DMO hydrogenation are EG and the main by-products are methyl glycolate (MG), EtOH, 2-methoxyethanol (2-ME), dimethyl ether (DME), 1,2-butanediol and 1,2-propanediol (named C3–4OH).

3 Results and Discussion

3.1 Hydroxyl Group Change of ZSM-5 Carrier

Sindorf et al. [26] have investigated the dehydration process of silica gel and they found that dehydroxylation could occur at 373 K, and the rate of dehydroxylation accelerated at ≥ 423 K, reaching a maximum speed at about 923 K. For the crystalline molecular sieves, the silanol groups possesses more unstable than that in the amorphous silicon due to the slight stress from the inclusion of silanol groups in the highly crystallized structures of zeolites [27], which further leads to easy dehydroxylation at lower temperatures. Thus, the process of dehydroxylation of zeolite molecular sieve can occur even at lower than 373 K, that is, the dehydroxylation reaction can occur just during the ordinary drying operation, which will inevitably affect the surface properties of the catalyst prepared later, but this point seems to be completely ignored by the researchers. In order to identify how the hydroxyl content affects the surface species of catalyst, the ZSM-5 zeolite was dried at 393 K for 0, 6 and 24 h, respectively, and FTIR of ZSM-5 after drying were conducted to determine the changes of hydroxyl content on the surface of ZSM-5. The results are shown in Fig. 1. As seen from Fig. 1a, the bands at 1110 and 800 cm^{-1} are assigned to asymmetric and symmetric stretching of the Si–O bonds in silica, respectively, and the shoulder peak at 960 cm^{-1} is ascribed to the vibration of surface -OH bonds. In order to accurately compare the changes of surface hydroxyl content, the relative amount of surface hydroxyl groups on the ZSM-5 can be calculated usually by normalizing the integrated intensity of the band at 960 cm^{-1} to that at 800 cm^{-1} (I_{960}/I_{800}) [28]. I_{960}/I_{800} values of ZSM-5 samples dried for different time are shown in Fig. 1b, and it can be clearly seen that the relative amount of surface hydroxyl groups decline with the increase of drying time. In addition, the decrease rate of relative amount of surface hydroxyl groups was faster in the early drying stage (such as 6 h), while the decrease rate is slowed down with the extension of drying time. This result directly confirmed that the ordinary drying process usually neglected by the researchers has a great influence on the surface properties of the carrier, rather than just "removing the adsorbed water".

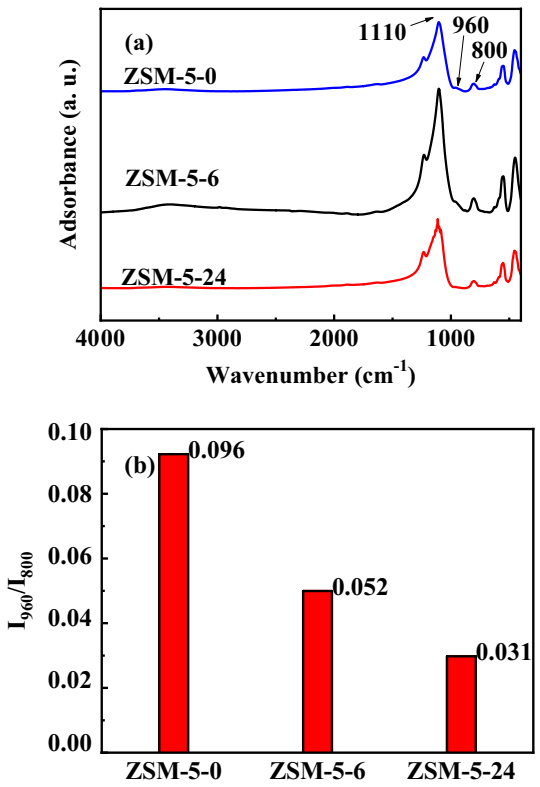

Fig. 1 FTIR spectra (**a**) and I_{960}/I_{800} ratios (**b**) of ZSM-5-N samples

3.2 Texture Properties of Calcined Cu/ZSM-5 Samples

Cu/ZSM-5 catalysts were prepared by ammonia evaporation of ZSM-5 carriers after drying at different time. The textural properties of calcined catalysts were characterized and the results are summarized in Table 1. The copper contents in all catalysts are same at 22–23%, thus it can be excluded the influence of copper loading. The relative amount of surface hydroxyl groups for ZSM-5 carriers decline after drying process and the BET surface areas of the subsequently prepared catalysts significantly increased. The BET surface areas of the catalyst prepared by ZSM-5 carrier without pre-drying are only 302 m^2/g, while that of the catalysts prepared after pre-drying are about 450 m^2/g. The main reason might come from two aspects: (1) the decreased number of hydroxyl groups on the support surface after the drying process led to the high dispersion and small particle size of copper species of the prepared Cu/ZSM-5 catalyst, which increased their surface areas; (2) the ammonia evaporation process for the pre-drying support reduced zeolite crystallinity and made more mesopores, in which the surface areas of prepared catalysts increased.

Figure 2 shows the XRD patterns of the calcined catalysts and ZSM-5 carrier without pre-drying, in which the peaks at 2θ = 5°–30° belong to ZSM-5 carrier and the peaks at 35.4° and 38.6° is corresponding to CuO crystallite (JCPDS05-0661). Cu/ZSM-5-0 sample exhibits high intensity of peaks for both ZSM-5 carrier and CuO crystallite, indicating that there are many large particles of CuO and high crystallinity ZSM-5 zeolite structure in the sample. However, the diffraction peaks for ZSM-5 are obviously weakened in Cu/ZSM-5-6 and Cu/ZSM-5-24 samples, and the peaks for CuO crystal are absence. Consideration that the instruments and test parameters used in the test process were exactly the same, the results above indicated that the interaction between copper and ZSM-5 was enhanced with the decrease of hydroxyl content, resulting in the destruction of ZSM-5 crystal structure (amorphous copper silicate was formed, which is discussed in detail below) and formation of small CuO particles with good dispersion.

The FT-IR technique was usually applied to identify the existence of copper phyllosilicate for the Cu/SiO_2 catalyst.

Table 1 Texture characteristics of calcined samples

Sample	W_{Cu} (wt%)[a]	S_{BET} (m^2/g)	V_p (cm^3/g)	d_p (nm)
ZSM-5	/	392	0.21	3.19
Cu/ZSM-5-0	23.20	302	0.24	6.26
Cu/ZSM-5-6	23.67	453	0.41	4.10
Cu/ZSM-5-24	22.11	449	0.40	4.16

[a]Determined by ICP-OES

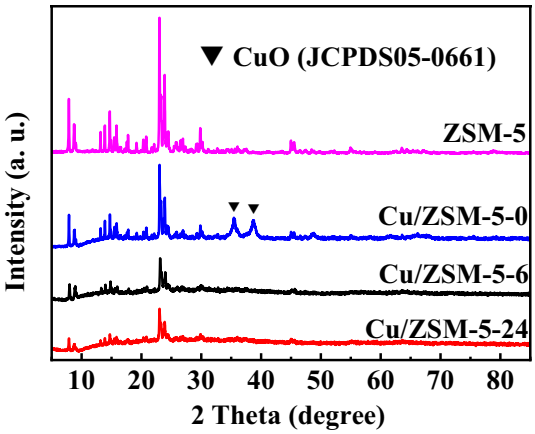

Fig. 2 XRD patterns of calcined Cu/ZSM-5-N samples

The bands at 800 cm^{-1} and 1110 cm^{-1} correspond to the ν_{SiO} asymmetric and ν_{SiO} symmetric stretching bands of SiO_2, respectively. The formation of copper phyllosilicate can be confirmed by two peaks, which are the characteristic δ_{OH} band at 670 cm^{-1} and the shoulder peak at 1040 cm^{-1} [25]. The surface hydroxyls of the silica [28], ammonia dosage[14] and ammonia evaporation temperature [1] might all play the important roles in the formation of copper phyllosilicate, but the actual process is very complex. Figure 3 shows the FTIR spectra of calcined samples in the frequency range of 400–4000 cm^{-1}. The bands at 1110, 800 and 470 cm^{-1} are assigned to different vibration modes of the Si–O bonds in the amorphous silica. The appearance of the δ_{OH} band at 670 cm^{-1} and the ν_{SiO} shoulder peak at 1040 cm^{-1} indicates the formation of copper phyllosilicate and the fitting content of the shoulder peak at 1040 cm^{-1} in the Cu/ZSM-5-6 and Cu/ZSM-5-24 are obviously higher than that in the Cu/ZSM-5-0 sample, indicating that the catalysts prepared with the pre-dried carrier is easier to form copper silicate phase than

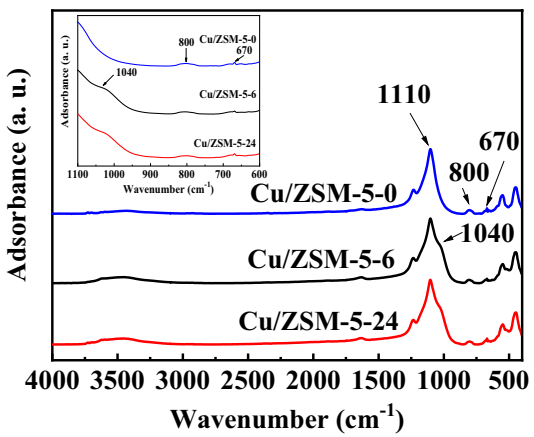

Fig. 3 FTIR spectra of calcined Cu/ZSM-5-N samples

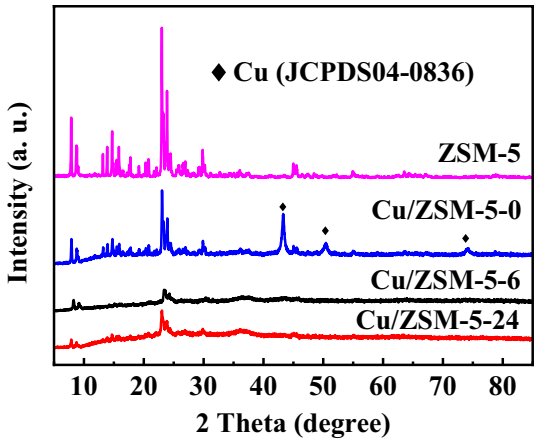

Fig. 4 XRD patterns of reduced Cu/ZSM-5-N samples

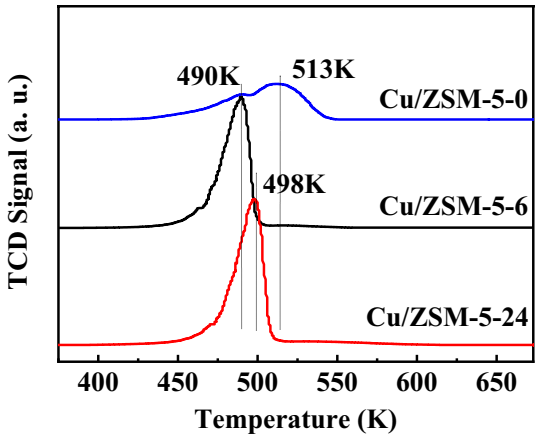

Fig. 5 H_2-TPR profiles of Cu/ZSM-5-N catalysts

that without pre-drying of the carrier. This result can well explain the decrease of ZSM-5 crystallinity in Cu/ZSM-5-6 and Cu/ZSM-5-24 samples obtained from the XRD pattern above. As copper species and silicon species formed a large number of copper silicate phases, the original crystal structure of molecular sieve is damaged, resulting in a significant reduction in the crystallinity of ZSM-5.

3.3 Types and Chemical States of Copper Species of Reduced Catalysts

Figure 4 shows the XRD diffraction pattern for the reduced catalysts and the CuO diffraction peaks (in Fig. 2 above) changes into a sharp diffraction peaks of metallic Cu ($2\theta = 43.3°$, 51.1° and 74.1°, JCPDS04-0836) for the Cu/ZSM-5-0 sample, indicating that the dispersion of copper particles is poor and there are a lot of large copper particles. However, no characteristic peak of Cu was detected in the catalysts prepared by pre-drying the support (Cu/ZSM-5-6 and Cu/ZSM-5-24), indicating that the Cu dispersions were higher and the copper particles were smaller after reduction in these two catalysts. The diffraction peaks corresponding to the ZSM-5 zeolite molecular sieve topology are still much weakened in Cu supported samples compared with that in the parent ZSM-5, due to the formation of a certain amount of copper phyllosilicate species which have been confirmed from the FTIR spectra above.

Figure 5 shows the H_2-TPR profiles of Cu/ZSM-5-N catalysts. The instruments, test parameters and the sample dosages used in the test process were exactly the same. The reduction temperatures for these catalysts exhibit great difference, which speculates the different contents of Cu–O–Si units in these catalysts. Kohler [29, 30] have been investigated the Cu/SiO_2 catalysts prepared by ion exchange method, two distinctly different copper species were identified: (1) the isolated copper atoms attached to two neighboring silanol groups (ion-exchanged) representing 10–25% of the copper loading, and (2) the remainder concentrated in numerous small copper particles, which derived from $Cu(OH)_2$ produced by pH reduction. The $Cu(OH)_2$ can analogously be form in the AE method, because the evaporation of ammonia also led to the decrement of the pH value of the suspension [1]. Toupance et al. [31] proposed that during the preparation of Cu/SiO_2 samples by copper complex and silica, two types of supported Cu^{2+} species (i.e., grafted Cu^{2+} ions and copper phyllosilicate) could be formed. The formation of grafted Cu^{2+} ions resulted from electrostatic adsorption of Cu^{2+} ammine complex in solution onto the surface of silica particles, also known as the ion exchange process; and the copper phyllosilicate formed in solution through the reaction between silicic acid arising from silica dissolution and copper complex. In addition, the signal intensities of H_2-TPR for Cu/ZSM-5-6 and Cu/ZSM-5-24 catalysts were higher than that for Cu/ZSM-5-0 catalyst, probably attributed to two aspects: (1) the Cu/ZSM-5-0 catalyst has a wider particle size distribution range, which makes the reduction peak widen and the strength decrease; (2) Cu/ZSM-5-0 catalyst might contain some copper species that are difficult to reduce under the current experimental conditions.

For the Cu/ZSM-5-0 sample, two reduction peaks at 490 K and 513 K could be observed. The peak at 490 K could be attributed to the reduction of the copper phyllosilicate and ion-exchanged Cu–O–Si units to Cu^+, while the peak at 513 K belongs to the large block CuO to metallic Cu, and the area of the latter peak is much larger than the former, indicating that large block CuO is dominant in Cu/ZSM-5-0 samples and the overall content of ion exchange Cu–O–Si phase and copper phyllosilicate is small [1]. However, the Cu/ZSM-5-6 and Cu/ZSM-5-24 exhibit much high and narrow reduction peaks at 490–498 K. The reduction temperature of Cu/ZSM-5-6 is consistent with that lower

reduction temperature of Cu/ZSM-5-0 (490 K), while that for Cu/ZSM-5-24 is slightly higher (498 K). These results indicate that Cu/ZSM-5-0 and Cu/ZSM-5-6 have the same origin of ion exchange Cu–O–Si units and copper phyllosilicate. Considering that there is only one reduction peak for the Cu/ZSM-5-6 and Cu/ZSM-5-24, it can be inferred with certainty that the range of reduction temperature also contains the reduction of highly dispersed CuO particles, for which the reduction temperature of CuO to Cu^0 in line with of Cu–O–Si units and copper phyllosilicate to Cu^+. The main reduction peak of Cu/ZSM-5-24 catalyst slightly moves to high temperature compared to that of Cu/ZSM-5-6 sample, which is consistent with the slightly larger particle sizes of Cu/ZSM-5-24 from the TEM analysis results below.

The TEM images of the reduced Cu/ZSM-5-N catalysts are shown in Fig. 6. Compared with the catalysts prepared by ZSM-5 without drying (Cu/ZSM-5-0), the copper particles of catalysts prepared by pre-drying the carrier (Cu/ZSM-5-6 and Cu/ZSM-5-24) have significantly more uniform distribution and smaller particle size of copper. The average sizes of copper nanoparticles for the three catalysts are 16.5, 5.0 and 7.9 nm, respectively, which are also in good agreement with the XRD results above. These results confirm again that the pre-drying process for the carrier have significant influence on the properties of the subsequent prepared Cu supported catalysts. It should be pointed out that although the carrier of Cu/ZSM-5-6 has more surface hydroxyl groups than Cu/ZSM-5-24, the copper particle size of the prepared catalyst is slightly smaller than the latter, indicating that the loaded copper species might be not change much when the number of hydroxyl groups decreases to a certain extent. Similar results can also be seen in the BET surface area of the catalysts mentioned above. For the Cu/ZSM-5-6 and Cu/ZSM-5-24, besides the uniformly distributed copper nanoparticles of about 5.0 and 7.9 nm (highlighted with red circles in the Fig. 6), it can be also seen that there are many extremely small Cu particles (highlighted with green circles in the Fig. 6), which might be attributable to some reduced copper phyllosilicate and Cu–O–Si units in the two samples. Thus, it can be proposed that the Cu species were supported in the ZSM-5 as three forms: copper phyllosilicate, Cu–O–Si units and deposited CuO particles. In addition, the particles with sizes of 5.0 and 7.9 nm were not detected in the XRD characterization, probably because they were the aggregate of many small Cu particles or amorphous copper silicate particles.

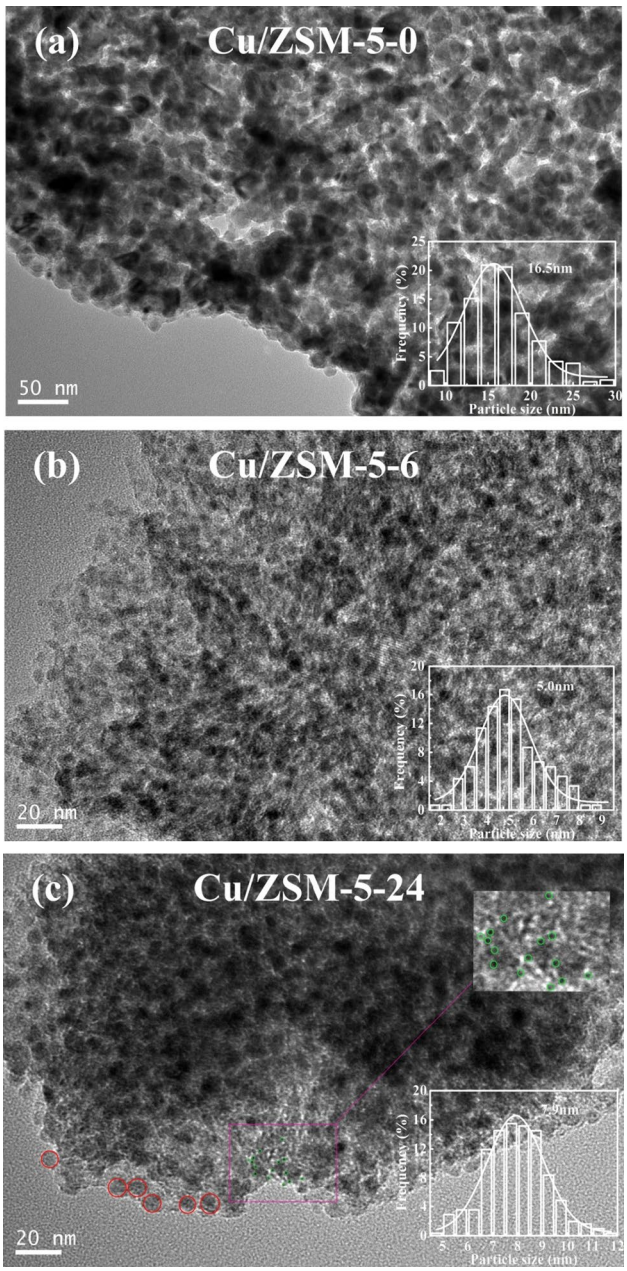

Fig. 6 TEM images of reduced Cu/ZSM-5-N samples

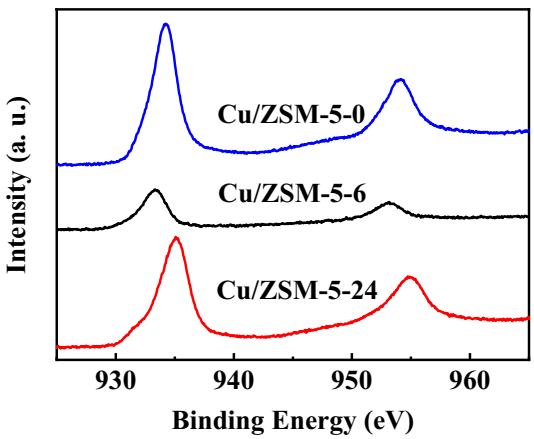

Fig. 7 Cu 2p XPS spectra of reduced Cu/ZSM-5-N catalysts

To further elucidate the surface chemical states in the reduced Cu/ZSM-5-N catalysts, the surface composition and valence state of copper was estimated by XPS characterization. XPS and XAES spectroscopy were conducted to measure the amounts of surface copper sites on the catalyst quantitatively. As shown in Fig. 7, the absence of satellite peak of binding energies (BE) at 942–944 eV indicates that Cu^{2+} species had been completely reduced to the lower state of Cu^{+} or Cu^{0}.

Generally, the BE of Cu^{0} and Cu^{+} at about 932.8 (Cu $2p_{3/2}$) and 952.8 eV (Cu $2p_{1/2}$) in XPS are almost the same, which cannot be distinguished only from Cu 2p XPS spectra, so further calculations depends on the XAES spectra [1]. In the Cu LMM XAES spectra of the catalysts prepared by three different pretreated supports, the peaks of BE are different (as shown in Fig. 8). The appearance of two obvious overlapping peaks at about 569.9 eV and 573.0 eV correspond to the existence of Cu^{0} and Cu^{+} species, respectively. The molar ratios of the surface $Cu^{+}/(Cu^{0}+Cu^{+})$, which is denoted as X_{Cu+}, could be determined by deconvolution of Cu LMM peaks and the result was summarized in Table 2. It can be seen that the X_{Cu+} value of Cu/ZSM-5-0 catalyst was 43.21%, while that for Cu/ZSM-5-6 and Cu/ZSM-5-24 was 50.20 and 47.02%, respectively, which are all higher than that of Cu/ZSM-5-0 catalyst, probably due to the high content of the copper phyllosilicate and Cu–O–Si units in the later two catalysts.

N_2O titration was carried out to investigate the Cu dispersion and the active specific surface area of Cu^{0}. The active specific surface area of Cu^{+} can be estimated based on the active surface area of Cu^{0} and the intensity ratio of $Cu^{+}/(Cu^{+}+Cu^{0})$ obtained from the results of the deconvolution of Cu LMM peaks above. The results are listed in Table 2. It can be seen that the dispersion of copper and the active specific surface area of Cu^{0} and Cu^{+} for the Cu/ZSM-5-6 and Cu/ZSM-5-24 catalysts are all much higher than that for the Cu/ZSM-5-0 catalyst (about twice). These results are in good agreements with TEM and XRD results.

Because the acidity of the catalyst is also an important factor affecting the catalytic performance of hydrogenation of DMO to EG, the NH_3-TPD characterization was carried out. As shown in Fig. 9, with the increase of temperature, there are three obvious desorption peaks at 423–523 K, 523–623 K and 823–923 K, corresponding to weak acid, medium strong acid and strong acid sites, respectively. For the three typical catalysts, it can be seen that with the decrease of hydroxyl content of the carrier, the strong acid sites disappears, and then the medium strong acid and weak acid increase first and then decrease. Due to the presence

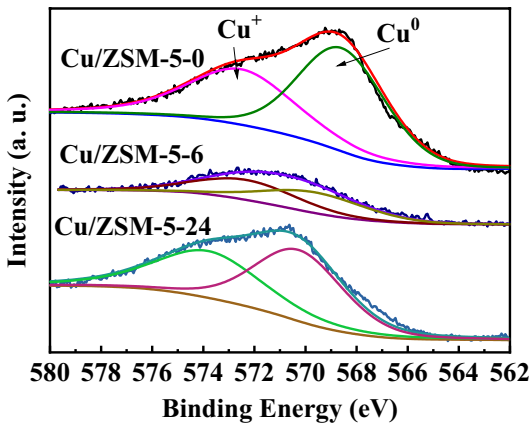

Fig. 8 Cu LMM XAES spectra of reduced Cu/ZSM-5-N catalysts

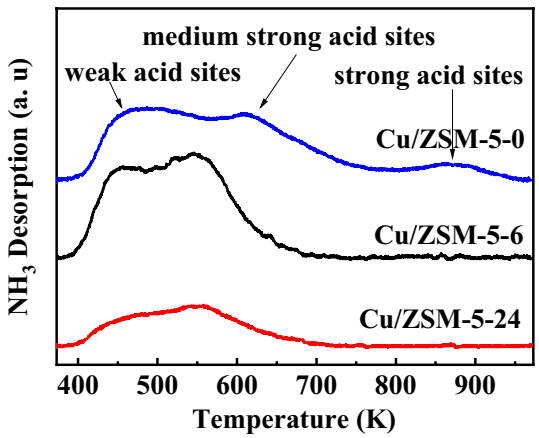

Fig. 9 NH_3-TPD spectra of Cu/ZSM-5-N catalysts

Table 2 Species and chemical composition of copper in Cu/ZSM-5-N samples

Sample	$Disp_{Cu}$ (%)[a]	S_{Cu0} (m^2/g)[b]	X_{Cu+} (%)[c]	D_{CuO} (nm)[d]	D_{Cu} (nm)[d]
Cu/ZSM-5-0	14.86	4.34	43.21	9.5	17.8
Cu/ZSM-5-6	28.35	8.12	50.20	ND[e]	ND
Cu/ZSM-5-24	23.32	7.15	47.02	ND	ND

[a,b]Determined by N_2O titration

[c]$Cu^{+}/(Cu^{+}+Cu^{0})$ is denoted as X_{Cu+} and calculated from Cu LMM XAES spectra

[d]Calculated by Scherrer formula from XRD results

[e]Not detected

Table 3 Catalytic performance of Cu/ZSM-5-N catalysts for hydrogenation of DMO

Catalyst	DMO Con. (%)	Sel. (%)					
		EtOH	MG	EG	2-ME	C3–4OH	Others
Cu/ZSM-5-0	52.12	/	82.17	/	15.8	/	2.03
Cu/ZSM-5-6	100	1.11	/	88.45	6.53	/	3.91
Cu/ZSM-5-24	100	1.25	0.89	93.04	/	2.11	2.71

Reaction conditions: 448 K, 2 MPa, $WLHSV_{DMO}=0.5\ h^{-1}$, $H_2/DMO=120$

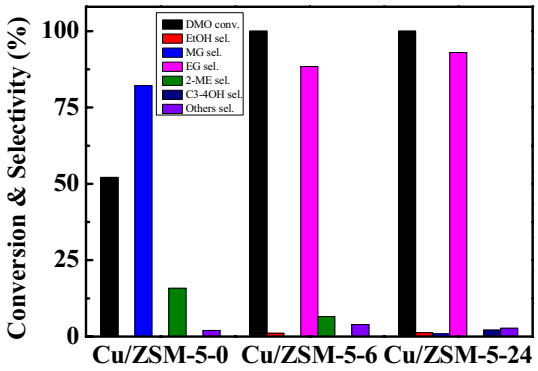

Fig. 10 Catalytic performances of Cu/ZSM-5-N catalysts for hydrogenation of DMO. Reaction conditions: 448 K, 2 MPa, $WLHSV_{DMO}=0.5\ h^{-1}$, $H_2/DMO=120$

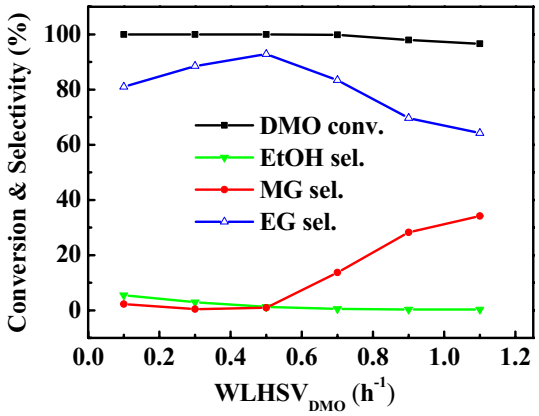

Fig. 11 Influence of $WLHSV_{DMO}$ on catalytic performance of Cu/ZSM-5-24 catalyst. Reaction conditions: 448 K, 2 MPa, $H_2/DMO=120$

of a small number of aluminum atoms in ZSM-5 molecular sieve, hydrogen ions around the aluminum atoms will migrate and form the bridge hydroxyl group of Al–OH–Si, which is the source of strong acid sites [32]. The bridge hydroxyl group would be broken and the strong acid sites transformed into weak and medium strong acid sites when molecular sieve was dried and dehydrated, thus the Cu/ZSM-5-6 possessed more weak and medium strong acid sites than the Cu/ZSM-5-0 sample. However, with the further drying, the terminal hydroxyl group also decreases, so the weak and medium strong acid sites in the Cu/ZSM-5-24 sample decreases accordingly.

3.4 Catalytic Activity Measurements and Analysis

The catalytic performances of Cu/ZSM-5-N catalysts were evaluated through the hydrogenation of DMO, and the results were shown in Table 3 and Fig. 10. It can be seen from Table 3, under the low temperature reaction condition of 448 K, the catalytic performance in the hydrogenation of DMO were profoundly affected by the change of hydroxyl amount of the carrier used. The conversion of DMO was only 52.12% over Cu/ZSM-5-0 catalyst prepared without pre-drying of the support and the product was mainly methyl glycolate (MG), indicating its low hydrogenation activity. However, DMO conversion over the Cu/ZSM-5-6 and Cu/ZSM-5-24 catalysts both reached 100% at 448 K and the selectivity of EG on the two catalysts was 88.45% and 93.04%, respectively. There were some differences in the distribution of by-products, with mainly 2-methoxyethanol (6.53%) over the Cu/ZSM-5-6 catalyst while C3–4OH (2.11%) over the Cu/ZSM-5-24 catalyst. Yue et al. [33, 34] believed that the strong acidic sites of the catalyst was the main reason for the intramolecular dehydration of ethylene glycol into ethanol, whereas the strongly basic sites catalyzed the Guerbet reaction to generate 1,2-butanediol (1,2-BDO) and 1,2-propanediol (1,2-PDO). In addition, MG could also be hydrogenated to methyl acetate, or react with methanol to produce methyl methoxy acetate. Zhu et al. [13] believed that dehydration between EG and methanol produced 2-methoxyethanol or intermolecular dehydration of methanol produced dimethyl ether on the catalysts acidic sites. Cu/SiO_2 was not favorable to the side reactions mentioned above due to the weak acidic and basic properties of SiO_2, and high EG selectivity could be obtained. The experimental results also confirm the above conclusion. Why the EG selectivity over Cu/ZSM-5-24 is higher than that of Cu/ZSM-5-6 catalyst will be discussed in detail in the next part of this paper.

The Cu/ZSM-5-24 catalyst exhibited the highest EG yield, so the effect of $WLHSV_{DMO}$ on the catalyst was further investigated under the conditions of reaction temperature 448 K, reaction pressure 2 MPa and hydrogen ester (H_2/

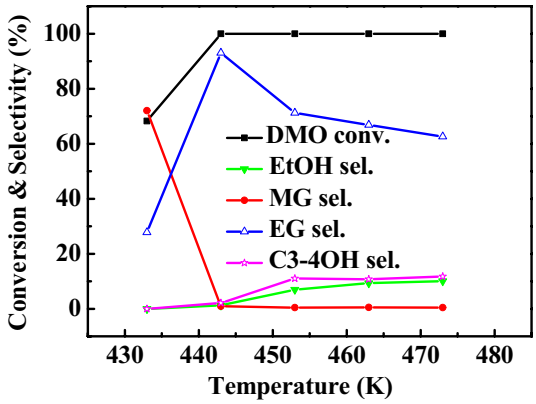

Fig. 12 Effect of reaction temperature on catalytic performance of Cu/ZSM-5-24. Reaction conditions: $WLHSV_{DMO}=0.5\ h^{-1}$, 2 MPa, $H_2/DMO=120$

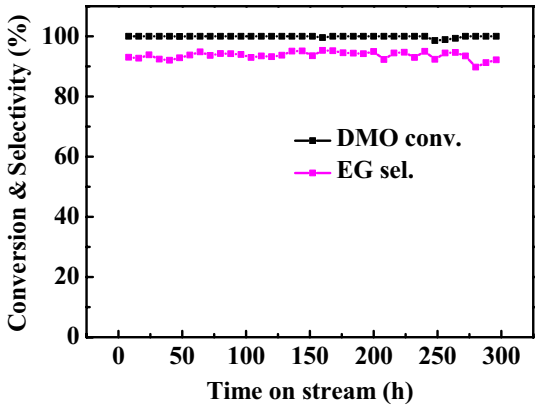

Fig. 13 Stability test of Cu/ZSM-5-24 catalyst. Reaction conditions: 448 K, 2 MPa, $WLHSV_{DMO}=0.5\ h^{-1}$, $H_2/DMO=120$

DMO) mole ratio 120. As shown in Fig. 11, the conversion of DMO decreased slowly when WLHSV was higher than 0.7, and it was still above 95% at WLHSV of 1.1. However, the EG selectivity presented a volcanic curve, and reached the maximum (92.8%) at WLHSV of 0.5, while MG selectivity showed a first decreasing and then increasing trend and it was the lowest at the WLHSV of 0.5.

Reaction temperature is also very important in catalytic reaction, and in literature the reaction temperature is mainly concentrated at about 473 K for the hydrogenation of DMO to EG. In this paper, the typical Cu/ZSM-5-24 catalyst toward DMO hydrogenation was investigated with respect to reaction temperature. As shown in Fig. 12, the DMO conversion always kept at 100% when the reaction temperature was higher than 448 K. DMO does not vaporize completely below its boiling point (436.5 K), but the DMO conversion still could reach nearly 70% at 433 K, indicating the high catalytic activity for the Cu/ZSM-5-24 catalyst. It should be noted that in the reported literature the conversion of DMO can reach 100% mostly under the reaction temperature at 473–493 K, thus the advantage of the catalytic activity of the catalysts in this paper should be highlighted. The selectivity of target product EG reached 93% at the low temperature of 448 K, and gradually decreased by increasing the reaction temperature, this is because of the increase of by-products with the increase of temperature, and indirectly reflects the high catalytic activity of the catalyst. Therefore, 448 K is preferred to be the best temperature over the catalyst. It is worth pointing out that there are few reports on the production of EG by DMO hydrogenation at low temperature [35]. Low temperature reaction can not only reduce energy consumption, but also greatly improve the stability of the catalyst, which has many advantages in industrial application.

The long-term stability of catalyst is of great significance for both industry and academia field. The result of catalytic stability test for Cu/ZSM-5-24 is shown in Fig. 13. DMO conversion and EG selectivity remained above 99% and 90% after 300 h over Cu/ZSM-5-24 catalyst. It has been reported in many literatures that the long-term stability of copper-silicon catalyst without promoter prepared by pure silicon carrier for hydrogenation of DMO is usually about 50–100 h [15, 18, 36]. It is generally believed that Hüttig and Taman temperatures of copper species in copper-silicon catalysts are lower than reaction temperature which led to the copper particles growing into larger crystallites through migration and coalescence of particles at high temperature, thus greatly reducing the dispersion of copper and the active surface area. That is the main reason for the easy inactivation of copper catalysts [33, 37]. In addition, methanol is both a common solvent and one of the products for the hydrogenation of DMO, which have also been proved to be another serious factor affecting the stability of Cu/SiO_2 catalyst. Wen et al. [38] investigated the deactivation mechanism of Cu/SiO_2 for the hydrogenation of DMO in methanol solvent. The reaction of SiO_2 with methanol leads to the loss of SiO_2 in the catalyst, which was an important reason for decreasing the copper surface area and the aggregation of copper particle, and further affected the activity and stability of the catalyst. Zheng et al. [39] focused on the effect of CO on the stability of Cu/SiO_2 in the reaction system, and proved that CO generated through methanol decomposition at the hydrogenation reaction temperature of DMO (473 K), would strongly adhere to Cu^+ sites, which destroyed the balance of active surface Cu^+ and Cu^0 species, and further induced Cu nanoparticles aggregation through the Ostwald ripening process. These two factors led to the irreversible deactivation of Cu/SiO_2 during the hydrogenation of DMO. In summary, the higher reaction temperature can prefer the aggregation of copper particles, the reaction of SiO_2 with methanol and the decomposition of methanol to generate CO, thus reducing the reaction temperature is a better choice to improve the

long-term stability of the Cu/SiO_2 catalyst. As compared to the other research achievements, the reaction temperature in this paper is greatly reduced. It will provide a basis for the new breakthrough of catalyst industrial production.

4 Discussion

Previous researchers have been systematically studied the reaction mechanism of DMO hydrogenation to EG over copper catalyst. Through experimental verification and theoretical calculation it has been proved that the equilibrium effect in the synergistic catalysis of Cu^0 and Cu^+ species was the key factor to realize the efficient hydrogenation of DMO. The synergistic catalytic mechanism of Cu^0 and Cu^+ species in ester hydrogenation reaction has been clarified, that is, Cu^0 species adsorbs and dissociates H_2, while the Cu^+ species adsorbs methoxy and acyl species [17] and could also act as electrophilic or Lewis acidic sites to polarize the C=O bond via the electron lone pair in oxygen [40]. Ma et al. [17] believed that the catalytic hydrogenation activity was determined by the number of Cu^0 species when the number of Cu^0 species was insufficient, but Cu^+ specific surface area plays a leading role in catalytic hydrogenation activity when Cu^0 species were abundant. The adsorption of ester is the control step of the reaction of DMO hydrogenation to EG.

4.1 Effect of Hydroxyl Groups on the Structure of Cu/ZSM-5-N Catalyst

The ammonia evaporation method for preparation of copper-silicon catalyst is a common method to increase the content of Cu^+ and the catalytic activity, and the reason might be attributed to two aspects. Firstly, the reaction of cuprammonia complex and silicon could form the copper phyllosilicate at a certain temperature in the preparation process of this method [1]. Secondly, the copper complex in the catalyst precursor was exchanged with hydroxyl on the silicon surface to form Cu–O–Si units [25, 31]. In the reduction process, the copper phyllosilicate and Cu–O–Si units were firstly reduced to Cu^+, but these Cu^+ species could be completely reduced to Cu^0 only at a higher temperature. Thus, there were a large amount of Cu^+ on the surface of the catalyst from the incomplete reduction of copper phyllosilicate and Cu–O–Si units, which was the main reason for the high activity of the catalyst [25]. In this study, it can be concluded that the change of hydroxyl group on the surface of the carrier has a significant impact on the structure and catalytic performance of the catalyst based on the results above. From the FT-IR results the hydroxyl content on the surface of the carrier can be effectively changed by the ordinary drying process. The effect of hydroxyl groups on the surface of the support on the structure of the subsequent prepared catalyst was further studied. It can be clearly seen from Fig. 3 and Table 2 that the content of copper phyllosilicate, dispersion of copper and the specific surface area of Cu^+ and Cu^0 in the catalyst prepared by the pre-dried support were all significantly higher than that of the catalyst prepared by the non pre-dried support. These results show that hydroxyl groups on the surface of the carrier could regulate the distribution and types of active centers. Previous researchers proposed that there are four main silanols (i.e., single, geminal, terminal, H-bonded hydroxyl groups) on the surface of SiO_2 [41], thus it can be inferred that over the Cu/ZSM-5-0 catalyst, hydroxyl groups on the surface of the support were mainly hydrogen-bonded hydroxyl groups, and only a small amount of single hydroxyl groups on the surface of the support could be exchanged with copper ions to form the Cu–O–Si units, while other large amount of copper ions exist in the form of large CuO particles. With the drying treatment of the carrier, most of the hydrogen-bonded hydroxyl groups were removed in the way of water molecules, and the surface of the carrier was dominated by the single-hydroxyl groups. During the preparation of the catalyst, a part of the copper was highly dispersed on the surface of the support by exchanging with two single-hydroxyl groups to form the copper phyllosilicate and Cu–O–Si units, which forms large amount of Cu^+ after the reduction process, and the other part was dispersed on the surface of the support in the form of small-sized copper particles. With further drying (ZSM-5-24), a large number of single-hydroxyl groups on the surface began to further disappear, and the remaining copper content after the exchange of copper ions with hydroxyl groups was higher than that of the copper species in the same form in the catalyst Cu/ZSM-5-6, making the particle size in Cu/ZSM-5-24 larger than that of the copper species in the Cu/ZSM-5-6 (Scheme 1).

The change of hydroxyl groups in the drying process can also influence another significant aspect, that is, the acidity of the catalyst. In the ZSM-5 zeolite, the strong acid was mainly contributed by the bridge hydroxyl group in the form of Al–OH–Si, and the medium strong acid was provided by the terminal hydroxyl group [42]. As the degree of drying progress, the elimination of aluminum hydroxyl groups led to the transformation of strong acid sites to the medium strong acid and weak acid sites. The quantitative and qualitative analysis of bridge hydroxyl groups is quite complicated, which is also the focus of our next research (i.e., how to quantitatively and qualitatively characterize the four hydroxyl groups). However, according to literature, the acidity of the silanol group on the surface of zeolite is generally higher than that of the hydroxyl group on the surface of amorphous silica [27]. Crépeau [32] demonstrated that the acidity of the hydroxide group could be strongly altered without significantly changing its tensile frequency. It is suggested that the free silanol group located near the

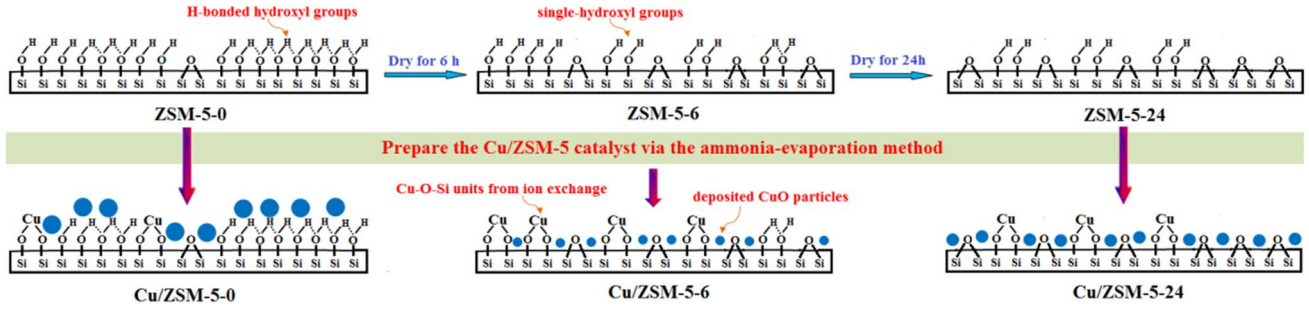

Scheme 1 The illustration for the possible structural change of surface hydroxyl groups of the ZSM-5 carrier under drying treatment and the structure of corresponding prepared Cu/ZSM-5-N catalysts

aluminum atom can show the same acidity as the bridged hydroxyl group, so the ZSM-5 is highly acidic when the surface environment is not dried. In addition, during the process of catalyst preparation, the lost bridged hydroxyl group could not regenerate in a short time due to the short contact time with water, but they could regenerate when the ZSM-5 was stored in a humid environment for a long time. In addition, the partial removal of H-bonded hydroxyl groups produced more single-hydroxyl groups and terminal hydroxyl groups, which was confirmed from the increase of medium strong acid content of Cu/ZSM-5-6 catalyst. With further drying, both single-hydroxyl and hydrogen bonds were removed to a certain extent, thus the content of the medium strong acid and weak acid sites decreased, which was also confirmed from the NH_3-TPD result of Cu/ZSM-5-24 catalyst.

4.2 The Relationship Between the Structure and Activity of Catalysts

It is well known that the hydrogenation process of DMO is a multi-step tandem reaction, which can generate a variety of by-products in the presence of acidic or alkaline sites, leading to the reduction of EG yield. The related reaction paths have been proposed based on different products. During the hydrogenation process of DMO, Cu^0 dissociates the adsorbed H_2 molecule and Cu^+ sites can act as electrophilic sites to polarize and activate the acyl group of the DMO reactant, thus Cu^+ and Cu^0 synergically catalyze the hydrogenation of DMO to EG [9]. The dissociation and adsorption of ester molecules is the rate controlling step in the hydrogenation of DMO. The results above show that the change of hydroxyl group on the surface of the carrier has significant effect on the structure and catalytic performance of the catalyst, mainly due to the effect of ion exchange of copper with surface hydroxyl groups on the dispersion of copper and the specific surface area of Cu^+ and Cu^0, which can directly influence the catalytic activities. The higher the hydroxyl content on the surface of the carrier, the more H-bonded hydroxyl groups, which is unfavorable to exchange with copper ions, thus reducing the dispersion of copper on the surface of the carrier. High X_{Cu+} and specific surface area of Cu^+ and Cu^0 are the key factors to have good catalyst activity at low temperature for the Cu/ZSM-5-6 and Cu/ZSM-5-24 catalysts. On the other hand, hydroxyl groups on the surface of the support can affect the acidity of the catalyst significantly. The acidity of Cu/ZSM-5-0 and Cu/ZSM-5-6 catalysts is the main factor for the formation of the by-products of ethers. For Cu/ZSM-5-0 catalyst, DMO in the methanol solution takes place multi-step reactions, which contain that (1) dimethyl ether (DME) is obtained by inter molecular dehydration of the methanol solvent on the strong acid sites; (2) MG and EG were obtained gradually with the hydrogenation of DMO on copper sites, which exhibits the low conversion of DMO due to the low copper dispersion of Cu/ZSM-5-0 catalyst; (3) the intermolecular dehydrating of EG and methanol on the medium strong acid sites to produce 2-methoxyethanol (2-ME). According to the previous literature [13] and experimental results, the reaction path of DMO on Cu/ZSM-5-N was summarized in scheme 2. For Cu/ZSM-5-6 catalyst, it has highest copper dispersion and the highest specific surface area of Cu^+ and Cu^0, resulting in good conversion of DMO, but it contains a large amount of medium strong acid, which leads to the production of 2-ME (6.53% of selectivity). As a result, EG selectivity is decreased. However, for the Cu/ZSM-5-24 catalyst, although the decline of hydroxyl group on the surface of the support leads to the copper dispersion decrease slightly, the decline of medium strong acid reduced the selectivity of the by-products, resulting in the high conversion of DMO (still 100%, due to the high copper dispersion) and the highest selectivity of EG (93%) among that over the three typical catalysts.

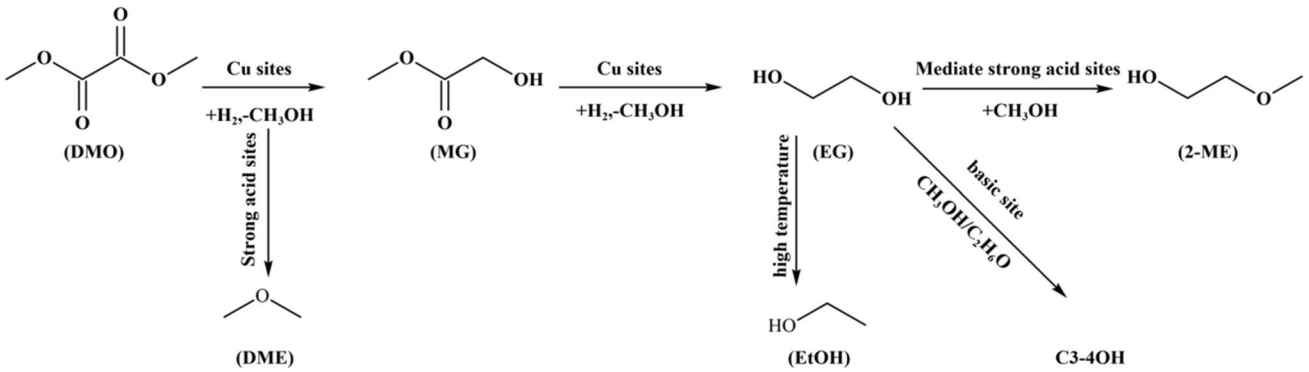

Scheme 2 Reaction network of the hydrogenation of DMO on Cu/ZSM-5-N catalysts

5 Conclusions

In this paper, ZSM-5 molecular sieve with very high Si/Al ratio was chosen as the probe carrier to prepare the Cu/ZSM-5 catalyst for the hydrogenation of DMO to EG. The hydroxyl content and type on the surface of the parent ZSM-5 carrier can be greatly changed during the ordinary drying process, which is often completely ignored by the researchers, but it has significant influence on the properties and catalytic activity of the subsequent prepared Cu/ZSM-5 catalyst. With the decrease of hydroxyl content on the surface of the ZSM-5 support from the continuous drying treatment of carrier, the prepared reduced Cu/ZSM-5 catalyst possessed smaller Cu particles size, higher copper dispersion, higher surface area of Cu^0 and Cu^+ species, but weakened surface acidity of the catalyst, which resulted in the great improvement of the catalytic performance in the hydrogenation of DMO to EG. The DMO conversion and EG selectivity could reach 100% and 93% even under the optimized low reaction temperature at 448 K over the Cu/ZSM-5-24 catalyst and the catalytic activity did not show obvious change after 300 h of reaction. These results are impressive and the influence of surface hydroxyl groups on the structure and surface chemistry of catalysts are explained scientifically, which would provide some theoretical and technical guidance for the design and synthesis of high activity catalysts in this direction.

Acknowledgements Financial supports from Key research and development program in Gansu Province (18YF1GA062), National natural science foundation of China (21763016) and Industrial support program for colleges and universities in Gansu Province (2020C-06) are acknowledged.

Declarations

Conflict of interest The authors declare that there is no conflict of interest.

References

1. Chen LF, Guo PJ, Qiao MH, Yan SR, Li HX, Shen W, Xu HL, Fan KN (2008) J Catal 257:172–180
2. Lin Q, Ji Y, Jiang ZD, Xiao WD (2007) Ind Eng Chem Res 46:7950–7954
3. Zhao YJ, Zhang YQ, Wang Y, Zhang J, Xu Y, Wang SP, Ma XB (2017) Appl Catal A Gen 539:59–69
4. Zhao XG, Lin Q, Xiao WD (2005) Appl Catal A Gen 284:253–257
5. Teunissen HT, Elsevier CJ (1997) Chem Commun 7:667–668
6. Guo XY, Yin AY, Dai WL, Fan KN (2009) Catal Lett 132:22–27
7. Han LP, Zhao GF, Chen YF, Zhu J, Chen PJ, Liu Y, Lu Y (2016) Catal Sci Technol 6:7024–7028
8. Hu Q, Fan GL, Yang L, Li F (2014) ChemCatChem 6:3501–3510
9. Kong XP, Chen Z, Wu YH, Wang RH, Chen JG, Ding LF (2017) RSC Adv 7:49548–49561
10. Kong XP, Zhang XC, Chen JG (2015) Catal Commun 65:46–50
11. Liu YT, Ding J, Bi JC, Sun YP, Zhang J, Liu KF, Kong FH, Xiao HC, Chen JG (2017) Appl Catal A Gen 529:143–155
12. Wang B, Wen C, Cui YY, Chen X, Dong Y, Dai WL (2015) RSC Adv 5:29040–29047
13. Zhu YF, Zhu YL, Ding GQ, Zhu SH, Zheng HY, Li YW (2013) Appl Catal A Gen 468:296–304
14. Li F, Lu CS, Li XN (2014) Chin Chem Lett 25:1461–1465
15. Lin JD, Zhao XQ, Cui YH, Zhang HB, Liao DW (2012) Chem Commun 48:1177–1179
16. Xu CF, Chen GX, Zhao Y, Liu PX, Duan XP, Gu L, Fu G, Yuan YZ, Zheng NF (2018) Nature Commun 9:3367–3376
17. Wang Y, Shen YL, Zhao YJ, Lv J, Wang SP, Ma XB (2015) ACS Catal 5:6200–6208
18. Zheng XL, Lin HQ, Zheng JW, Duan XP, Yuan YZ (2013) ACS Catal 3:2738–2749
19. Wang Y, Zhao YJ, Lv J, Ma XB (2017) ChemCatChem 9:2085–2090
20. Perret N, Wang XD, Delgado JJ, Blanco G, Chen XW, Olmos CM, Bernal S, Keane MA (2014) J Catal 317:114–125
21. Huang Y, Ariga H, Zheng XL, Duan XP, Takakusagi S, Asakura K, Yuan YZ (2013) J Catal 307:74–83
22. Yin AY, Wen C, Guo XY, Dai WL, Fan KN (2011) J Catal 280:77–88
23. Zhang CC, Wang DH, Dai B (2017) Catalysts 7:122
24. Yin AY, Guo XY, Fan KN, Dai WL (2010) ChemCatChem 2:206–213
25. Ding J, Popa T, Tang J, Gasem KAM, Fan M, Zhong Q (2017) Appl Catal B Environ 209:530–542
26. Sindorf DW, Maciel GE (1983) J Am Chem Soc 105:1487–1493

27. Kondo JN, Yoda E, Ishikawa H, Wakabayashi F, Domen K (2000) J Catal 191:275–281
28. Wang Y, Yang WL, Yao DW, Wang SP, Xu Y, Zhao YJ, Ma XB (2020) Catal Today 350:127–135
29. Kohler MA, Curry-Hyde HE, Hughes AE, Sexton BA, Cant NW (1987) J Catal 108:323–333
30. Kohler MA, Lee JC, Trimm DL, Cant NW, Wainwright MS (1987) Appl Catal 31:309–321
31. Toupance T, Kermarec M, Lambert JF, Louis C (2002) J Phys Chem B 106:2277–2286
32. Crépeau G, Montouillout V, Vimont A, Mariey L, Cseri T, Maugé F (2006) J Phys Chem B 110:15172–15185
33. Yue HR, Ma XB, Gong JL (2014) Acc Chem Res 47:1483–1492
34. Yue HR, Zhao YJ, Ma XB, Gong JL (2012) Chem Soc Rev 41:4218–4244
35. Zhao Y, Kan X, Yun HF, Wang DL, Li N, Li GX, Shen JY (2021) Catal Commun 154:106310
36. Ma XB, Chi HW, Yue HR, Zhao YJ, Xu Y, Lv J, Wang SP, Gong JL (2013) AIChE J 59:2530–2539
37. Zhao YJ, Kong LX, Xu YX, Huang HJ, Yao YQ, Zhang JW, Wang SP, Ma XB (2020) Ind Eng Chem Res 59:12381–12388
38. Wen C, Cui YY, Dai WL, Xie SH, Fan KN (2013) Chem Commun 49:5195–5197
39. Zheng JW, Zhou JF, Lin HQ, Duan XP, Williams CT, Yuan YZ (2015) J Phys Chem C 119:13758–13766
40. Li SM, Wang Y, Zhang J, Wang SP, Xu Y, Zhao YJ, Ma XB (2015) Ind Eng Chem Res 54:1243–1250
41. Wang RW, Wunder SL (2000) Langmuir 16:5008–5016
42. Sulpizi M, Gaigeot MP, Sprik M (2012) J Chem Theory Comput 8:1037–1047

Publisher's Note Springer Nature remains neutral with regard to jurisdictional claims in published maps and institutional affiliations.